Pflugers Arch - Eur J Physiol (2013) 465:1041–1049
DOI 10.1007/s00424-013-1230-3

SENSORY PHYSIOLOGY

Effects of cholesterol alterations are mediated via G-protein-related pathways in outer hair cells

Takahiko Nagaki · Seiji Kakehata · Rei Kitani · Takahisa Abe · Hideichi Shinkawa

Received: 12 November 2012 / Revised: 27 January 2013 / Accepted: 28 January 2013 / Published online: 17 February 2013

Abstract Cholesterol is an essential component of cell membranes, and determines their rigidity and fluidity. Alterations in membrane cholesterol by MβCD or water-soluble cholesterol affect the stiffness, capacitance, motility, and cell length of outer hair cells (OHCs). This suggests that reconstruction of the cytoskeleton may be induced by cholesterol alterations. In this study, we investigated intracellular signaling pathways involving G proteins to determine whether they modulate the changes in voltage-dependent capacitance caused by cholesterol alterations. Membrane capacitance of isolated guinea pig OHCs were assessed using a two-sine voltage stimulus protocol superimposed onto a voltage ramp (200 ms duration) from −150 to +140 mV. One group of OHCs was treated with 100 μM guanosine 5′-*O*-(3-thiotriphosphate) tetralithium salt (GTPγS), the GTP analog, administrated into individual cells via patch pipettes. Another group of OHCs was internally perfused with 600 μM guanosine 5′-(β-thio) diphosphate trilithium salt (GDPβS), the GDP analog. A third group was perfused with internal solution only as a control. Application of 1 mM MβCD shifted non-linear capacitance curves to the depolarized direction of the control group with reduction of the peak capacitance (C_{mpeak}). After the 10-min application of MβCD, shifts of voltage at C_{mpeak} (V_{cmpeak}) and reduction of C_{mpeak} were 73.32±11.09 mV and 9.09±2.10 pF, respectively (n=4). On the other hand, in the GTPγS-treated group, the shift of V_{cmpeak} and reduction of C_{mpeak} were attenuated remarkably. The shift of V_{cmpeak} and reduction of C_{mpeak} in the 10-min application of MβCD were 9.73± 10.92 mV and 3.08±1.91 pF, respectively (n=7). MβCD decreased the cell length by 16.53±4.27 % in the control group and by 6.45±6.22 % in the GTPγS group. In addition, we investigated the effects of GDPβS on cholesterol-treated OHCs. One millimolar cholesterol was externally applied after the 4-min application of 1 mM MβCD because the shift of V-C_m function caused by cholesterol alone was small. Application of cholesterol shifted V-C_m curves of the control group to the hyperpolarized direction with increase of the C_{mpeak}. After the 10-min application of cholesterol, changes of V_{cmpeak} and C_{mpeak} were −9.19±6.68 mV and 2.14±0.44 pF, respectively (n=4). On the other hand, in the GDPβS-treated OHCs, the shift of V_{cmpeak} and increase of C_{mpeak} were attenuated markedly. The shift of V_{cmpeak} and increase of C_{mpeak} after 10 min were 5.13±10.46 mV and −0.55±1.39 pF, respectively (n=6). This study demonstrated that internally perfused GTPγS inhibited the MβCD effects and GDPβS inhibited the cholesterol effects, raising the possibility that G proteins may be involved in outer hair cell homeostasis as well as the possibility that cholesterol response may be G protein mediated. More study is required to clarify the detailed role of G proteins in the relation between cholesterol and the OHC cytoskeleton.

Keywords Cholesterol · Outer hair cell · Electromotility · Membrane capacitance · Cochlear amplifier · Methyl-beta-cyclodextrin · Guanosine 5′-*O*-(3-thiotriphosphate) tetralithium salt · Guanosine 5′-(β-thio) diphosphate trilithium salt · G protein

Abbreviations

OHC	Outer hair cell
MβCD	Methyl-beta-cyclodextrin

T. Nagaki · S. Kakehata · R. Kitani · T. Abe · H. Shinkawa
Department of Otorhinolaryngology, Hirosaki University School of Medicine, 5 Zaifu-cho,
Hirosaki 036-8562, Japan

S. Kakehata (✉)
Department of Otolaryngology Head and Neck Surgery, Yamagata University Faculty of Medicine, 2-2-2 Iida Nishi,
Yamagata 990-9585, Japan
e-mail: seijik06@gmail.com

NLC	Nonlinear capacitance
C_m	Membrane capacitance
C_{mpeak}	Peak capacitance
V_m	Membrane potential
V_{cmpeak}	Voltage at peak capacitance
Q_{max}	Maximal charge movement
z	Valence
C_{lin}	Linear membrane capacitance
GTPγS	Guanosine 5′-*O*-(3-thiotriphosphate) tetralithium salt
GDPβS	Guanosine 5′-(β-thio) diphosphate trilithium salt

Introduction

Outer hair cells (OHCs) elongate and shorten in response to electrical, mechanical, or chemical stimulation. These motile responses are crucial components of the cochlear amplifier which provide frequency selectivity and sensitivity of mammalian hearing [2, 3, 16, 36]. While OHCs' electromotile responses arise from the motor protein, prestin, a modified anion exchanger [4, 9–11, 40, 41], actin-spectrin cytoskeleton lying beneath the plasma membrane helps maintain the cell shape and modulate the electromotility as well as contribute to the fine-tuning of the acoustic transduction process [3, 7]. These layers of OHCs' lateral wall are connected together by "pillars" that play a role in the interaction between the plasma membrane and cytoskeleton (cortical lattice) [7, 39]. OHC electromotility is variable by many factors; intracellular turgor pressure, osmolarity, temperature, electrical field, drugs, and so on [17, 18, 23].

Cholesterol is an essential component of cell membranes, and determines their rigidity and fluidity. It is suggested that the cholesterol levels in the plasma membrane can affect the efficiency of the motor protein [1, 8, 37]. Changes in cholesterol level in the plasma membrane using methyl-β-cyclodextrin (MβCD) or water-soluble cholesterol affect the membrane capacitance, cell motility, stiffness, and cell length of OHCs [29, 33]. This suggests that cytoskeletal reorganization could be associated with membrane cholesterol levels. The Rho (Ras homologous) family of small GTPases plays a crucial role in cytoskeletal reorganization and mediates different types of motility by regulating the actin polymerization and depolymerization in nonauditory cell populations. Small GTPases RhoA, Rac1, and cdc42 have been identified as regulators of OHC motility [20]. In this study, we investigated intracellular signaling pathways involving G proteins to determine whether they modulate the cell changes derived by cholesterol alteration.

Materials and methods

Isolation of cells

Guinea pigs of both sexes, weighting 200–400 g, were anesthetized by intraperitoneal administration of pentobarbital sodium (30 mg/kg) and sacrificed by decapitation in accordance with the Guidelines for Animal Experimentation, Hirosaki University. The organ of Corti was removed from each cochlear spiral and incubated with tripsin for 10 min. OHCs were isolated using a 50-μl Hamilton syringe and suspended in external solution (15 ml) before being observed with an inverted microscope (Olympus IX71N) and recorded by digital video camera (SONY HDR-SR11). Cell lengths were measured from recorded images (Adobe Photoshop).

Whole-cell patch clamp

Whole-cell voltage-clamp was achieved with conventional patch techniques [14, 19]. Patch electrodes were made from borosilicate capillary glass (G-1.5; Narishige, Tokyo, Japan) using a P-97 micropipette puller (Sutter Instruments, Novato, CA). The intrapipette solution (blocking solution) for capacitance measurements consisted of (in mM): 140 CsCl, 2 $MgCl_2$, 10 EGTA, 10 HEPES, pH of which adjusted to 7.2 with Tris. The standard external solution contained (in mM): 100 NaCl, 20 TEA, 20 CsCl, 2 $CoCl_2$, 1.52 $MgCl_2$, 10 HEPES, the pH of which was adjusted to 7.2 with Tris. The osmolarity of these solutions was adjusted to 300 mOsm with glucose. OHCs were whole-cell voltage clamped with an Axon 200B amplifier using patch pipettes having initial resistances of 3–5 MΩ. Series resistances ranged from 5 to 20 MΩ [26, 27]. All data acquisition and analysis were performed with a Windows-based patch clamp program, jClamp. After the membrane rupture, OHCs were kept in whole-cell mode at least 5 min before performing experiments to permit the cells to reach their mechanical equilibrium [25]. Experiments were done at room temperature.

Measurement of membrane capacitance

Membrane capacitance was assessed using a two-sine voltage stimulus protocol superimposed onto a voltage ramp (200 ms duration) from −150 to +140 mV. Capacitance data were fit to the first derivative of a two-state Boltzmann function [12, 35, 36].

$$Q_{(v)} = \left(\frac{Q_{\max}}{1 + \exp\left[-ze\left(V_m - V_{\text{peakcm}}\right)/kT\right]} \right) + Q_{\min}$$

Where Q_{max} is the maximum non-linear charge moved, V_{cmpeak} is voltage at peak capacitance or half maximum

charge transfer, V_m is membrane potential, z is valence, C_{lin} is linear membrane capacitance, e is electron charge, k is Boltzmann's constant, and T is absolute temperature.

Drugs

MβCD (methyl beta cyclodextrin Sigma; Sigma, C4555) is one of the family of cyclic oligomers of glucose, well known to remove cholesterol selectively from large unilamellar vesicles of various compositions [5]. In this study, MβCD was used to remove cholesterol from OHC plasma membrane [8, 32, 38]. Water-soluble cholesterol (cholesterol-methyl-beta-cyclodextrin/cholesterol-MβCD) (Sigma, C4951): a powder that is soluble in water at 200 mg/ml, contains approximately 40 mg of cholesterol per gram, and balanced with MβCD, was used to deliver cholesterol to OHC membrane [34]. These drugs were dissolved in external solution (1 mM) and applied continuously (1 ml/min) by the use of a multi barrel system (VC-6, Warner Instrument Corp. Hamden, USA). The tip of the multi barrel was located about 5 mm from the cell, permitting immediate exchange of the solution around the cell. One group of OHCs was treated with 100 μM guanosine 5′-*O*-(3-thiotriphosphate) tetralithium salt (GTPγS, Sigma G8634): G-protein activating analog of guanosine triphosphate (GTP) administered into the cell via patch pipettes. Another group of OHCs was treated in the same manner with 600 μM guanosine 5′-(β-thio) diphosphate trilithium salt (GDPβS, Sigma G7637)/GDP analog and generally used as a G-protein inhibitor. The third group was administered with internal solution only as a control. External perfusion buffer was delivered around the cells continuously (1 ml/min).

Statistical analysis

All data are shown as mean ± the standard deviation. The p value was analyzed by Mann–Whitney test, with $p<0.05$ being considered statistically significant.

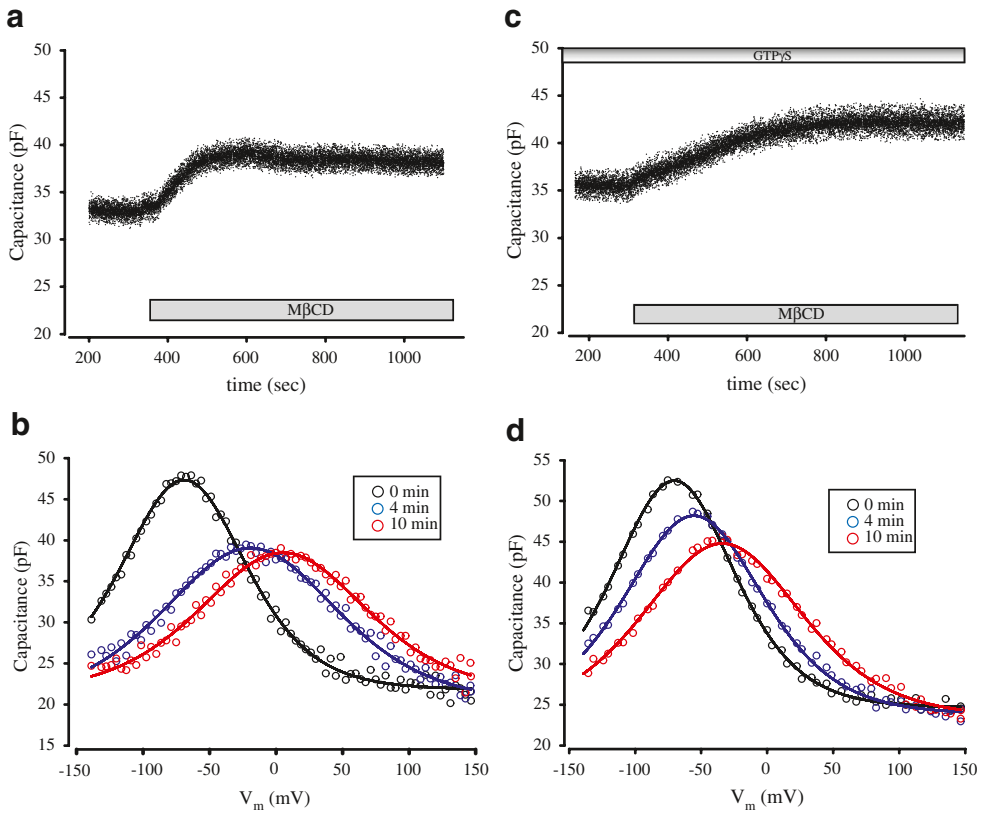

Fig. 1 GTPγS inhibits the effect of MβCD. **a**, **c** Continuous measurement of C_m at 0 mV. **b**, **d** Measurement of membrane capacitance using a two-sine voltage stimulus protocol. **a**, **b** Control cells: *Horizontal bar* indicates application of 1 mM MβCD. Immediately after the MβCD delivery, capacitance at 0 mV increased, followed by a slow decrease. This reflects the shift of non-linear capacitance to the depolarized direction (**a**). V_{cmpeak}/C_{mpeak} at 0, 4, and 10-min application of MβCD were −63.93 mV/47.91 pF, −22.68 mV/39.48 pF and 3.57 mV/39.04 pF. V_{cmpeak} shifted to the depolarized direction and C_{mpeak} decreased markedly (**b**). **c**, **d** GTPγS administered cells: OHCs were internally perfused with 100 mM GTPγS. After 7 min of whole cell configuration, 1 mM MβCD was delivered externally. MβCD application did not cause immediate capacitance change (**c**). V_{cmpeak}/C_{mpeak} at 0, 4, and 10-min application of MβCD were −60.29 mV/52.32 pF, −56.53 mV/48.69 pF, and −33.99 mV/45.69 pF (**d**)

Results

GTPγS inhibits the effect of MβCD

OHCs possess voltage-dependent nonlinear capacitance (NLC), which mirrors the charge movement in prestin and is characteristic of voltage-sensor activity. To study the effects of depleting cholesterol in the plasma membrane on NLC and cell shape, MβCD, which is known to remove the cholesterol in the plasma membrane, was applied by the use of a multi barrel system. Figure 1a shows a representative capacitance change at 0 mV induced by external application of MβCD. Immediately after the MβCD delivery, capacitance at 0 mV increased followed by a slow decrease. Figure 1b shows the changes of voltage-C_m (V-C_m) function measured by the same cell precisely before (0 min) and during extracellular application of 1 mM MβCD (4 min, 10 min) using a two-sine voltage stimulus protocol. MβCD application for 10 min shifted voltage at peak capacitance (V_{cmpeak}) to the depolarized direction by 67.5 mV and at the same time decreased peak capacitance (C_{mpeak}) by 8.87 pF.

To see the effects of G protein in the cholesterol depletion process, 100 μM GTPγS was internally applied. GTPγS itself did not change the V-C_m function up to 10 min (n=3: data not shown). Figure 1c shows an effect of external application of MβCD on capacitance of OHCs internally perfused with 100 μM GTPγS. After the MβCD delivery, capacitance at 0 mV increased slowly. Figure 1d shows the changes of the V-C_m function measured in the same cell at 0, 4, and 10 min after the application of MβCD. V_{cmpeak} was shifted to the depolarized direction by 26.3 mV, and C_{mpeak} decreased 6.63 pF at 10 min. These results indicate that effects of MβCD were attenuated by GTPγS.

Figure 2a–c show the average changes in V_{cmpeak}, C_{mpeak}, and cell length up to 10 min with and without internally perfused GTPγS, respectively. The shifts of the V_{cmpeak} and the C_{mpeak} decrease were inhibited in the GTPγS-treated group. The shifts of the V_{cmpeak} and the C_{mpeak} decreases at each point were statistically significant (p<0.05). After the 10-min application of MβCD, the V_{cmpeak} shifts of the control (n=4) and GTPγS-treated groups (n=7) were 72.32±11.09 and 9.73±10.92 mV, respectively, and the C_{mpeak} decrease of the control and GTPγS groups were 9.09±2.10 pF and 3.08±1.91 pF, respectively. The cell length of the control group decreased immediately while the length decrease of the GTPγS-treated group was inhibited. The results of 1, 5, 8, and 10 min showed that the length decreases at each point were statistically significant (p<0.05). After the 10-min application of MβCD, cell length change of the control and GTPγS-treated groups were 16.53±4.27 and 6.45±6.22 %, respectively.

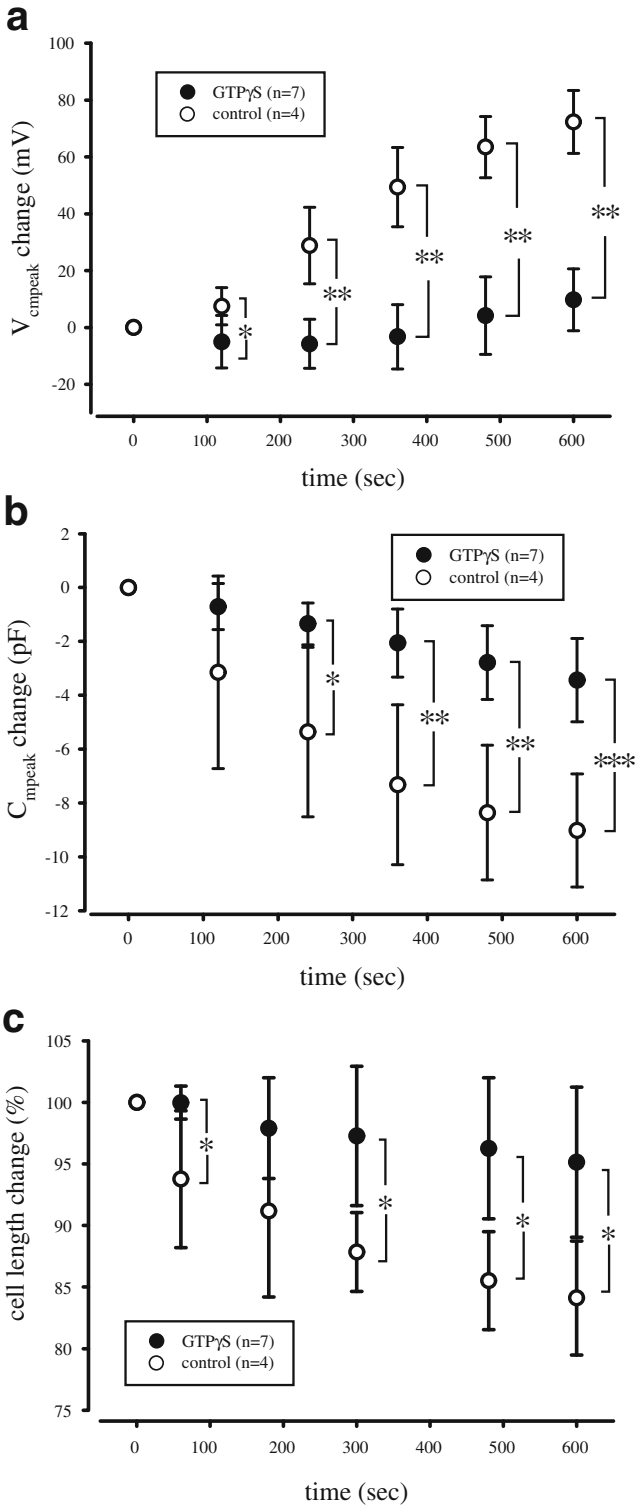

When OHCs were treated with GDPβS by the same protocol, no statistical changes in V_{cmpeak} and C_{mpeak} were seen between GDPβS-treated cells and control cells (Fig. 3a, b).

◀ **Fig. 2** **a** Inhibition of MβCD-induced changes in V_{cmpeak} by GTPγS. The V_{cmpeak} of the control group shifted to the depolarized direction after the MβCD application, while the voltage shifts of the GTPγS-treated group were inhibited. The results of 4 to 16 min showed that voltage shifts at each point were statistically significant ($p<0.05$). After the 10-min application of MβCD, V_{cmpeak} shifts of the control ($n=4$) and GTPγS groups ($n=7$) were 72.32±11.09 and 9.73±10.92 mV, respectively. (*$p<0.05$, **$p<0.01$). **b** Inhibition of MβCD-induced changes in C_{mpeak} by GTPγS. The C_{mpeak} of the control group decreased after the MβCD application, while the decreases of the GTPγS-treated group were inhibited. The result of 4 to 10 min showed that the C_{mpeak} decreases at each point were statistically significant ($p<0.05$). After the 10-min application of MβCD, C_{mpeak} shifts of the control and GTPγS groups were −9.09±2.10 pF and −3.08±1.91 pF, respectively. (*$p<0.05$, **$p<0.03$, ***$p<0.01$). **c** Inhibition of MβCD-induced changes in cell length by GTPγS. The cell length of the control group decreased immediately while the length decrease of the GTPγS group was inhibited. The results of 1, 5, and 10 min showed that the length decreases at each point were statistically significant ($p<0.05$). After the 10-min application of MβCD, cell length change of the control and GTPγS groups were 16.53±4.27 % and 6.45 ±6.22 %, respectively (*$p<0.05$)

GDPβS inhibits the effect of cholesterol

In reverse, the effects of loading cholesterol in the plasma membrane were tested by water-soluble cholesterol (cholesterol-MβCD). Rajagopalan et al. demonstrated that loading excess cholesterol shifted V_{cmpeak} toward hyperpolarizing voltages after depletion of cholesterol shifted V_{cmpeak} in the depolarizing direction [32, 33]. To clarify the effects of cholesterol on C_m, MβCD was applied for 4 min before application of the cholesterol, because the shift of V-C_m function caused by cholesterol alone was small and time course of the voltage shift was variable.

Continuous measurement of C_m at 0 mV showed that 1 mM water-soluble cholesterol shifts the C_m in the opposite direction of MβCD (Fig. 4a). V-C_m function was measured using a two-sine voltage stimulus protocol before cholesterol application, and 6, 10 min application of cholesterol (Fig. 4b). After the 10-min cholesterol application, V_{cmpeak} was shifted to the hyperpolarized direction by 7.68 mV, and the C_{mpeak} increased 2.83 pF.

OHCs administered with GDPβS showed different results. Figure 4c shows a representative C_m change of OHC internally perfused with 600 μM GDPβS. Application of MβCD increased the C_m at 0 mV immediately as in the control cells without 600 μM GDPβS. However, switching to cholesterol did not cause obvious changes of C_m at 0 mV. V-C_m function shows that the shift of V_{cmpeak} and decrease of C_{mpeak} are much smaller than those in the control cells after the 10-min application of cholesterol. The V_{cmpeak} was shifted to the depolarized direction by 3.84 mV, and C_{mpeak} decreased 0.42 pF after the 10-min application of cholesterol (Fig. 4d).

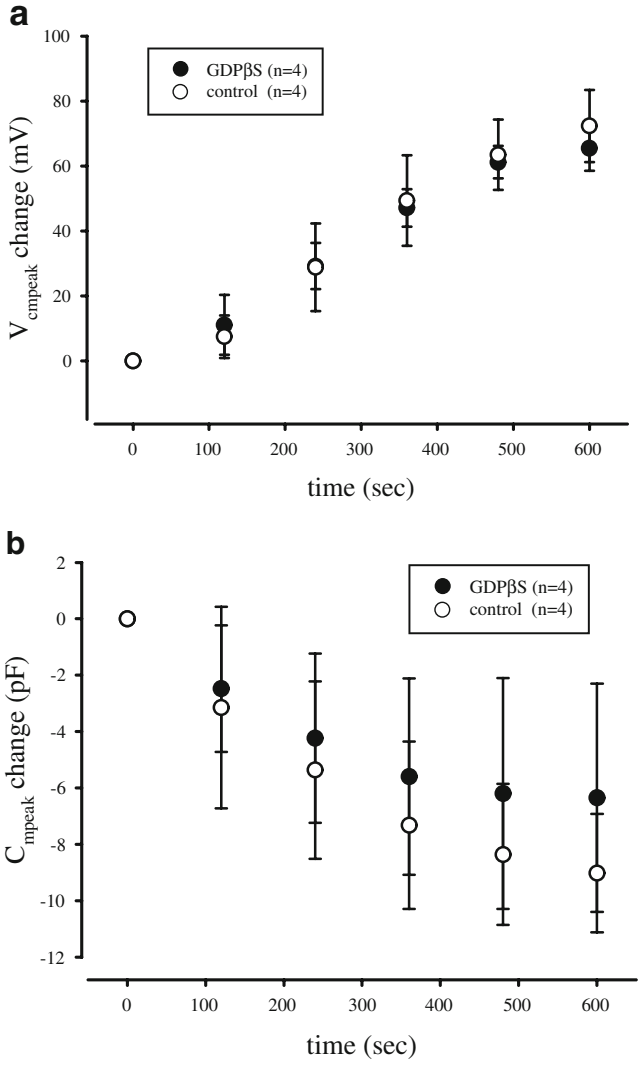

Fig. 3 **a**, **b** No inhibition of MβCD-induced changes in V_{cmpeak} and C_{mpeak} by GDPβS. OHCs were treated with GDPβS by the same protocol as GTPγS, then no statistical changes in V_{cmpeak} and C_{mpeak} were seen between GDPβS-treated cells and control cells. After the 10-min application of MβCD, V_{cmpeak} shifts of the control ($n=4$) and GDPβS groups ($n=4$) were 72.32±11.09 and 65.43±6.85 mV, respectively and C_{mpeak} shifts of the control and GDPβS groups were −9.09± 2.10 and −6.35±4.05 pF, respectively

Figure 5a and b show the average changes in V_{cmpeak} and C_{mpeak} up to 10 min with and without internally perfused GDPβS. The shifts of the V_{cmpeak} and the C_{mpeak} increase were inhibited in the GDPβS-treated group. The shifts of the V_{cmpeak} and the C_{mpeak} decreases at each point were statistically significant ($p<0.05$). After the 10-min application of cholesterol, the V_{cmpeak} shifts of the control ($n=4$) and GDPβS-treated groups ($n=6$) were −9.19±6.68 and 5.13±10.46 mV, respectively, and the C_{mpeak} change of the control and GDPβS-treated groups were 2.14±0.44 pF and −0.55±1.39 pF, respectively.

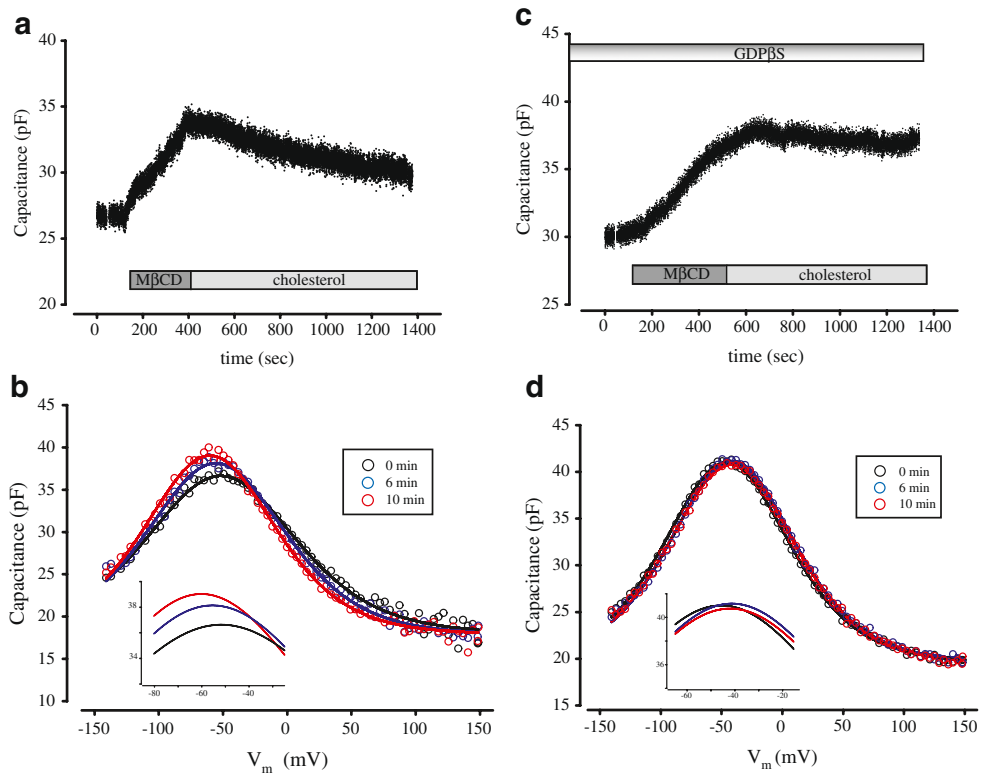

Fig. 4 GDPβS inhibits the effect of cholesterol. To clarify the effects of cholesterol on C_m, MβCD was applied for 4 min before application of the cholesterol, because the time course of the voltage shift caused by cholesterol alone was small. **a**, **c** Continuous measurement of C_m at 0 mV. *Horizontal bar* indicates application of 1 mM MβCD and 1 mM cholesterol. **b**, **d** Measurement of membrane capacitance using a two-sine voltage stimulus protocol. **a**, **b** Control cells: application of MβCD increased the capacitance at 0 mV immediately, and switching to cholesterol decreased the capacitance (**a**). V_{cmpeak}/C_{mpeak} at 0-, 6-, and 10-min application of cholesterol were −53.94 mV/37.17 pF, −61.62 mV/38.86 pF, and −61.62 mV/40.00 pF. V_{cmpeak} shifted to the hyperpolarized direction and C_{mpeak} increased (**b**). **c**, **d** GDPβS administered cells: application of MβCD increased the capacitance at 0 mV immediately as in the control cells. However, switching to cholesterol did not cause obvious decrease of capacitance (**c**). V_{cmpeak}/C_{mpeak} at 0-, 6-, and 10-min application of cholesterol were −50.10 mV/41.15 pF, −50.10 mV/41.37 pF, and −46.26 mV/40.95 pF (**d**)

Discussion

Cholesterol alteration of OHC membrane induces changes of the stiffness, capacitance, motility, and cell length [7, 29, 31]. The effects of MβCD application on capacitance are quite similar to those of increasing the membrane tension [17]. This similarity suggests that depleting cholesterol may decrease the rigidity of both plasma membrane and cortical lattice, resulting in increase of tension in the less rigid plasma membrane. Indeed, our preliminary data showed that externally applied MβCD reduced stiffness of the OHCs [24]. Huang et al. indicated that cell shape change caused by intracellular trypsin treatment itself did not affect the NLC [15]. Kakehata et al. also demonstrated that the OHCs treated by trypsin showed no change of C_{mpeak} and V_{cmpeak} in constant pressure [17]. However, based on these results, the dramatic effects of MβCD on OHCs are difficult to explain only by the membrane tension change. The electromechanically evoked cell movements and the prestin-associated currents are modulated by agents that alter the material properties of the membrane and cholesterol has been known to alter membrane material properties. In the present paper, we showed that a decrease in outer hair cell length as cholesterol was removed from the membrane (Fig. 2c) for the first time although mechanism of how to maintain the outer hair cell length remained to be explored.

To explain the mechanism of capacitance, motility, and cell length changes caused by MβCD, we focused on G protein. The results of the present study raise the possibility that G proteins may be involved in outer hair cell homeostasis as well as the possibility that cholesterol response is G protein mediated. Membrane-associated G proteins are involved in numerous signaling cascades. When the cholesterol in the membrane changes, it is likely that compensatory homeostatic mechanism that maintains the prestin-associated charge movement and cell length at their initial values work. Our results using the GTP and GDP analogues suggest that G protein facilitates the compensatory homeostatic mechanism in OHCs.

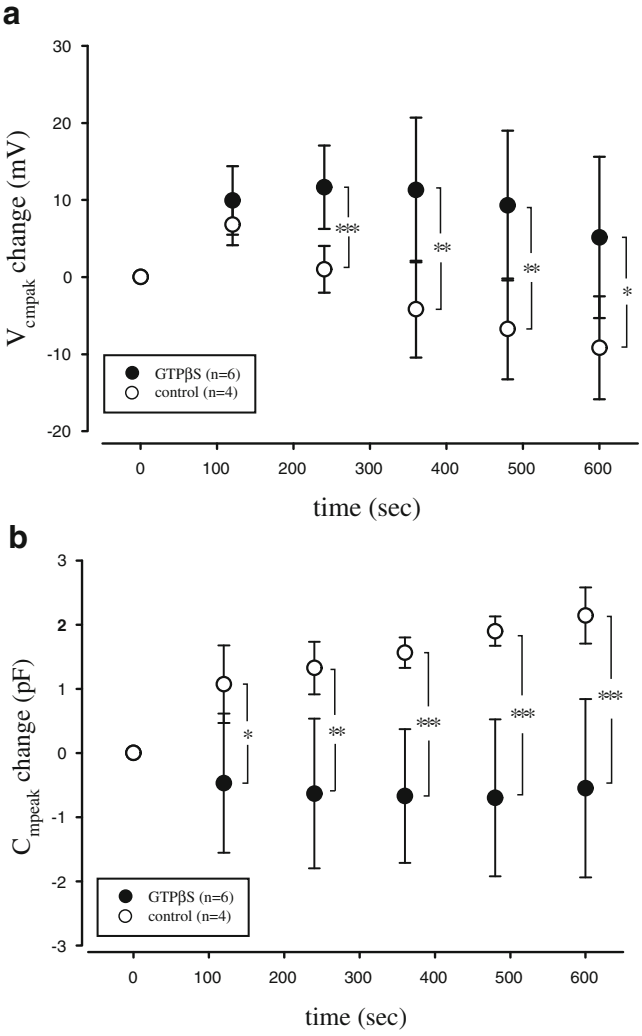

Fig. 5 **a** Inhibition of cholesterol-induced changes in V_{cmpeak} by GDPβS. The V_{cmpeak} of the control group shifted to the hyperpolarized direction after the cholesterol application, while the shifts of the GDPβS-treated group were inhibited. The results of 4 to 10 min showed that the differences in the shift at each point were statistically significant ($p<0.05$). After the 10-min application of cholesterol, V_{cmpeak} shifts of the control ($n=4$) and GDPβS ($n=6$) groups were −9.19±6.68 and 5.13±10.46 mV, respectively. (*$p<0.05$; **$p<0.03$; ***$p<0.01$). **b** Inhibition of cholesterol induced changes in C_{mpeak} by GDPβS. The C_{mpeak} of the control group increased after the cholesterol application, while the increases of the GDPβS-treated group were inhibited. The results of 2 to 10 min showed that there were statistically significant differences in the shift at each point ($p<0.05$). After the 10-min application of cholesterol, C_{mpeak} shifts of the control and GDPβS groups were 2.14±0.44 pF and −0.55±1.39 pF, respectively. (*$p<$ 0.05; **$p<0.03$; ***$p<0.01$)

In addition the compensatory homeostatic mechanism, the reorganization of the membrane–cytoskeleton complex might be involved in these changes. G protein is known to regulate the actin turnover via intracellular signaling pathways [6, 13, 30, 42]. Small GTPases such as RhoA, Rac1, and cdc42 are proved to be expressed in guinea pig OHCs and regulate the motility [20]. In this study, GTPγS (GTP analog), known to induce the actin polymerization [21], was administered via patch pipette to activate the GTPases. As a result, administration of GTPγS suppressed the effect of MβCD. On the other hand, administration of GDPβS (GDP analog), which is known to inactivate GTPases, suppressed the effect of water-soluble cholesterol. These results suggest that G-protein-mediated intracellular signaling pathways may regulate the OHC's cytoskeletal reconstruction triggered by cholesterol alteration, although detailed mechanisms remain to be demonstrated.

In general, RhoA, Lac1, and cdc42 are well known to play crucial roles in stress fiber formation, lamellipodia, and filopodia, respectively. These are the important processes of cell movement such as migration and division in nonauditory cells [13, 20]. However, OHCs are highly differentiated and have lost their faculties of migration and division. As the expected substitute ability, they can change their length and adjust the function of cochlear amplification depending on the biotic condition (e.g., hyperlipidemia, dehydration, and so on) [31]. Several lines of evidence indicate that small GTPases may be adapted to regulation of cytoskeletal reconstruction. Pivola et al. demonstrated that the c-Jun-N-terminal kinase (JNK) pathway is associated with stress, injury, and apoptosis of OHCs, and blocking the activation of this pathway protects the OHCs from noise trauma and aminoglycoside toxicity [30]. Bodmer et al. demonstrated that small GTPases are to be the upstream activator of the JNK pathway in OHCs [6]. These results show that small GTPases plays a crucial role of regulating the cytoskeletal reorganization and maintenance in OHCs. Recent study also indicates lipid rafts regulate the actin cytoskeleton by intracellular signaling pathways in T-cells [28]. However, precise roles of lipid rafts, which regulate the actin cytoskeleton in OHCs remain to be demonstrated.

The possibilities raised in this study should be investigated by several experiments. Histological experiments using a photomicrogram would detect the changes in F-actin in GTPγS-treated OHCs. Indeed, Khatibzadeh recently reported that F-actin depolymerization reduces the effect of cholesterol depletion on membrane mechanics, suggesting the possibility that cortical lattice may directly influence outer hair cell membrane mechanics [22]. The change in cytoskeletal–membrane interactions mechanics with change in cholesterol concentration is consistent with the change in prestin function observed in the present study. Measurement of the membrane stiffness in GTPγS-treated OHCs by atomic force microscopy would enhance the result. It is also necessary to investigate the involved G-protein-mediated intracellular signaling pathways. Effects of selective antagonists for small GTPs such as toxin B from *Clostridium difficile* (specific inhibitor of RhoA, Rac1, and Cdc42), exoenzyme C3 from *C. difficile* (specific RhoA inhibitor), and dominant negative of Rac1 and Cdc42 (dnRac1 and

dnCdc42) would enhance the results. Constitutively activated mutants of the small GTPases (RhoAQL, Rac1QL, and Cdc42QL) also should be tried. The results of these agents would demonstrate the possibility of participation of small GTPases in the signaling pathways.

Conclusion

In conclusion, this study suggested that intracellular signaling pathways involving G proteins might play role in cholesterol alteration process. More study is required to clarify the detailed role of G proteins in the relation between cholesterol and the OHC cytoskeleton.

Acknowledgments This work was supported by a Grant-in-Aid for Scientific Research from the Ministry of Education, Science and Culture of Japan (S.K). The authors would like to thank Ms. A. C. Apple-Mathews for valuable suggestions concerning English usage.

References

1. Abe T, Kakehata S, Kitani R, Maruya S, Navaratnam D, Santos-Sacchi J, Shinkawa H (2007) Developmental expression of the outer hair cell motor prestin in the mouse. J Membr Biol 215:49–56
2. Ashmore J, Avan P, Brownell WE, Dallos P, Dierkes K, Fettiplace R, Grosh K, Hackney CM, Hudspeth AJ, Julicher F, Lindner B, Martin P, Meaud J, Petit C, Sacchi JR, Canlon B (2010) The remarkable cochlear amplifier. Hear Res 266:1–17
3. Ashmore J (2008) Cochlear outer hair cell motility. Physiol Rev 88:173–210
4. Belyantseva IA, Adler HJ, Curi R, Frolenkov GI, Kachar B (2000) Expression and localization of prestin and the sugar transporter GLUT-5 during development of electromotility in cochlear outer hair cells. J Neurosci 20:116
5. Beseničar M, Bavdek A, Kladnik A, Maček P, Anderluh G (2007) Kinetics of cholesterol extraction from lipid membranes by methyl-β-cyclodextrin: a surface plasmon resonance approach. Biochim Biophys Acta 1778:175–184
6. Bodmer D, Brors D, Pak K, Gloddek B, Ryan A (2002) Rescue of auditory hair cells from aminoglycoside toxicity by *Clostridium difficile* toxin B, an inhibitor of the small GTPases Rho/Rac/Cdc42. Hear Res 172:81–86
7. Brownell WE, Spector AA, Raphael RM, Popel AS (2001) Micro- and nanomechanics of the cochlear outer hair cell. Annu Rev Biomed Eng 3:169–194
8. Brownell WE, Jacob S, Hakizimana P, Ulfendahl M, Fridberger A (2011) Membrane cholesterol modulates cochlear electromechanics. Pflugers Arch - Eur J Physiol 461:677–686
9. Dallos P (2008) Cochlear amplification, outer hair cells and prestin. Curr Opin Neurobiol 18:370–376
10. Dallos P, Wu X, Cheatham MA, Gao J, Zheng J, Anderson CT, Jia S, Wang X, Cheng WH, Sengupta S, He DZ, Zuo J (2008) Prestin-based outer hair cell motility is necessary for mammalian cochlear amplification. Neuron 58:333–339
11. He DZZ, Zheng J, Kalinec F, Kakehata S, Santos-Sacchi J (2006) Tuning in to the amazing outer hair cell: membrane wizardry with a twist and shout. J Membr Biol 209:119–134
12. Homma K, Dallos P (2010) Evidence that prestin has at least two voltage-dependent steps. J Biol Chem 286:2297–2307
13. Jiang H, Sha SH, Schacht J (2006) Rac/Rho pathway regulates actin depolymerization induced by aminoglycoside antibiotics. J Neurosci Res 83(8):1544–1551
14. Horn R, Marty A (1988) Muscarinic activation of ionic currents measured by a new whole-cell recording method. J Gen Physiol 92:145–159
15. Huang G, Santos-Sacchi J (1994) Motility voltage sensor of the outer hair cell resides within the lateral plasma membrane. Proc Natl Acad Sci U S A 91:12268–12272
16. Kachar B, Brownell WE, Altschuler R, Fex J (1986) Electrokinetic shape changes of cochlear outer hair cells. Nature 322:365–8
17. Kakehata S, Santos-Sacci J (1995) Membrane tension directly shifts voltage dependence of outer hair cell motility and associated gating charge. Biophys J 68:2190–2197
18. Kakehata S, Santos-Sacchi J (1996) Effects of salicylate and lanthanides on outer hair cell motility and associated gating charge. J Neurosci 16:4881–4889
19. Kalinec F, Holley MC, Iwasa KH, Lim DJ, Kachar B (1992) A membrane-based force generation mechanism in auditory sensory cells. Proc Natl Acad Sci U S A 89:8671–8675
20. Kalinec F, Zhang M, Urrutia R, Kalinec G (2000) Rho GTPases mediate the regulation of cochlear outer hair cell motility by acetylcholine. Biochemistry 275:28000–28005
21. Katanaev V, Wymann M (1998) GTPgamma S-induced actin polymerisation in vitro: ATP- and phosphoinositide-independent signalling via Rho-family proteins and a plasma membrane-associated guanine nucleotide exchange factor. J Cell Sci 111:1583–1594
22. Khatibzadech K, Gupta S, Farrell B, Brownell WE, Anvari B (2012) Effects of cholesterol on nano-mechanical properties of the living cell plasma membrane. Soft Matter 8:8350–8360
23. Kitani R, Kakehata S, Kalinec F (2011) Motile responses of cochlear outer hair cells stimulated with an alternating electrical field. Hear Res 280:209–218
24. Kitani R, Kakehata S, Murakoshi M, Wada H, Maruya S, Abe T, Shinkawa H (2008) The direct effects of cholesterol and Mβcd on outer hair cell motility and capacitance. ARO abstract828
25. Matsumoto N, Kalinec F (2005) Prestin-dependent and prestin-independent motility of guinea pig outer hair cells. Hear Res 208:1–13
26. Matsumoto N, Kitani R, Maricle A, Mueller M, Kalinec F (2010) Pivotal role of actin depolymerization in the regulation of cochlear outer hair cell motility. Biophys J 99:2067–2076
27. Matsumoto N, Kitani R, Kalinec F (2011) Linking LIMK1 deficiency to hyperacusis and progressive hearing loss in individuals with Williams syndrome. Commun Integr Biol 4:208–210
28. Meri F (2005) Lipid rafts and regulation of the cytoskeleton during T cell activation. 360:1663–1672
29. Nguyen TV, Brownell WE (1998) Contribution of membrane cholesterol to outer hair cell lateral wall stiffness. Otolaryngol Head Neck Surg 119:14–20
30. Pivola U, Xing-Qun L, Virkkala J, Saarma M, Murakata C, Camoratto M, Walton K, Ylikoski J (2000) Rescue of hearing, auditory hair cells, and neurons by CEP-1347/KT7515, an inhibitor of c-Jun N-terminal kinase activation. 20(1):43–50
31. Preyer S, Baisch A, Bless D, Gummer AW (2001) Distortion product otoacoustic emissions in human hypercholesterolemia. Hear Res 152:139–151
32. Rajagopalan L, Greeson JN, Xia A, Liu H, Sturm A, Raphael RM, Davidson AL, Oghalai JS, Pereira FA, Brownell WE (2007) Tuning of the outer hair cell motor by membrane cholesterol. J Biol Chem 282:36659–36670

33. Rajagopalan L, Organ-Darling LE, Liu H, Davidson AL, Raphael RM, Brownell WE, Pereira FA (2010) Glycosylation regulates prestin cellular activity. J Assoc Res Otolaryngol 11:39–51
34. Rong J, Shapiro M, Trogan E, Fisher E (2003) Transdifferentiation of mouse aortic smooth muscle cells to a macrophage-like state after cholesterol loading. Proc Natl Acad Sci U S A 100:13531–13536
35. Santos-Sacci J (1991) Reversible inhibition of voltage-dependent outer hair cell motility and capacitance. J Neurosci Off J Soc Neurosci 100:13531–13536
36. Santos-Sacci J (2003) New tunes from Corti's organ: the outer hair cell boogie rules. Curr Opin Neurobiol 13:459–468
37. Sfondouris J, Rajagopalan L, Pereira FA, Brownell WE (2008) Membrane composition modulates prestin-associated charge movement. J Biol Chem 283:22473–22481
38. Sturm AK, Rajagopalan L, Yoo D, Brownell WE, Pereira FA (2007) Functional expression and microdomain localization of prestin in cultured cells. Otolaryngol Head Neck Surg 136:434–439
39. Tolomeo J, Steele C, Holley M (1996) Mechanical properties of the lateral cortex of mammalian auditory outer hair cells. Biophys J 71:421–429
40. Wang A, Yang S, Jia S, He DZ (2010) Prestin forms oligomer with mechanically independent subunits. Brain Res 33:28–35
41. Zheng J, Shen W, He DZ, Long KB, Madison LD, Dallos P (2000) Prestin is the motor protein of cochlear outer hair cells. Nature 405:149–155
42. Zigmond S, Joyce M, Borleis J, Bokoch G, Devreotes P (1997) Regulation of actin polymerization in cell-free systems by GTPgS and Cdc42. J Cell Biol 138:363–374